Revista de Ciencias Tecnológicas (RECIT). Universidad Autónoma de Baja California ISSN 2594-1925
Volumen 9 (3): e502. Julio-Septiembre, 2026. https://doi.org/10.37636/recit.v9n3e502

Research article

Design, fabrication and experimental evaluation of a three-finger Fin Ray soft gripper

Diseño, fabricación y evaluación experimental de una pinza blanda de tres dedos tipo Fin Ray

Hoang Bui Huy

VNU University of Engineering and Technology, Vietnam National University, Hanoi, Vietnam. E-mail: hoangbh86@vnu.edu.vn. ORCID: 0009-0002-3446-210X.

Received: July 8, 2026 **Accepted:** July 30, 2026 **Published:** August 8, 2026

Abstract.- *This study presents the design, finite element analysis, fabrication, and experimental validation of a low-cost three-finger soft gripper based on the Fin Ray effect. The proposed system integrates TPU 95A compliant fingers, a PLA supporting structure, and an Arduino-controlled stepper-motor actuation mechanism. Several Fin Ray rib configurations were systematically evaluated using analytical modelling, finite element simulations, and experimental testing under a representative 5 N loading condition. The results showed that the contact region located approximately between one-half and two-thirds of the finger length produced the most effective deformation behavior. Among the investigated configurations, the curved-rib design achieved the largest displacement of approximately 14.45 mm while maintaining stable grasping performance. Good agreement was obtained between numerical predictions and experimental measurements, with deformation errors generally below 10% and a maximum error of 11.22%. The study establishes a reproducible CAD–FEA–3D printing experimental validation workflow and demonstrates a low-cost Fin Ray soft gripper platform that can support future research, rapid prototyping, and engineering education.*

Keywords: Soft gripper; Fin Ray effect; Additive manufacturing; TPU; Finite element simulation; Experimental validation; Robotic grasping.

Resumen.- *Este estudio presenta el diseño, el análisis por elementos finitos, la fabricación y la validación experimental de una pinza blanda de tres dedos de bajo coste basada en el efecto Fin Ray. El sistema propuesto integra dedos flexibles de TPU 95A, una estructura de soporte de PLA y un mecanismo de accionamiento mediante motor paso a paso controlado por Arduino. Se evaluaron sistemáticamente varias configuraciones de nervaduras Fin Ray utilizando modelos analíticos, simulaciones por elementos finitos y ensayos experimentales bajo una condición de carga representativa de 5 N. Los resultados mostraron que la zona de contacto situada aproximadamente entre la mitad y los dos tercios de la longitud del dedo producía el comportamiento de deformación más eficaz. Entre las configuraciones estudiadas, el diseño con nervaduras curvas logró el mayor desplazamiento —aproximadamente 14,45 mm— manteniendo al mismo tiempo un rendimiento de agarre estable. Se obtuvo una buena concordancia entre las predicciones numéricas y las mediciones experimentales, con errores de deformación generalmente inferiores al 10 % y un error máximo del 11,22 %. El estudio establece un flujo de trabajo reproducible de validación experimental (CAD-FEA-impresión 3D) y demuestra la viabilidad de una plataforma de pinza blanda Fin Ray de bajo coste que puede servir de apoyo para futuras investigaciones, la creación rápida de prototipos y la enseñanza de la ingeniería.*

Palabras clave: Pinza blanda; Efecto Fin Ray; Fabricación aditiva; TPU; Simulación por elementos finitos; Validación experimental; Agarre robótico.

1. Introduction

Soft robotics has become an important research direction for robotic manipulation because compliant structures can interact safely with uncertain environments and objects with variable shape, stiffness, and surface condition. Compared with rigid end effectors, soft grippers distribute contact deformation over larger areas and reduce local pressure, which is particularly relevant for food handling, agricultural manipulation, biomedical tools, and service robots [1]-[5].

Within this field, the Fin Ray effect offers a simple passive mechanism for adaptive grasping. A ribbed triangular finger bends toward the applied contact force rather than away from it, enabling the finger to wrap around curved or irregular surfaces without requiring a fully articulated mechanism or complex sensing system. Previous studies have demonstrated Fin Ray based soft grippers, 3D printed Fin Ray fingers, finite-element optimization, and analytical modelling for compliant manipulation [6]-[10].

Recent research has also moved beyond empirical design toward data driven prediction, tactile integration, and structural optimization of Fin Ray fingers. Physics informed neural networks, reconfigurable tactile grippers, learning based finger design, and layer jamming Fin Ray fingers have been proposed to improve deformation prediction, grasp stability, and task adaptability [11]-[14].

Additive manufacturing is closely related to this design direction because it allows fast iteration of rib geometry and direct fabrication of compliant or semi compliant structures. Studies on soft matter printing, 3D printing of soft robotic systems, soft robot manufacturing, and soft robotic materials show that material selection, process anisotropy, and fabrication parameters strongly influence the final mechanical response of soft grippers [15]-[18].

Other soft robotic and compliant grasping approaches provide useful design principles for the present work. Elastomeric soft systems, fiber reinforced bending actuators, fluidic elastomer robots, underactuated hands, and granular jamming grippers show that mechanical compliance can reduce control complexity while maintaining practical grasping capability [19]-[23].

Application oriented studies further indicate that soft grippers can be adapted for biomedical manipulation, stiffness adjustable systems, general soft manipulators, and small-scale robotic actuation. These studies emphasize the need to balance compliance, load capacity, repeatability, and safe interaction with fragile objects [24]-[27].

Recent work on self-healing soft robots, electroadhesive soft grippers, and comparative evaluations of soft-gripper technologies also highlights the importance of durability, contact control, and application specific actuation selection. These issues motivate the present low-cost Fin Ray gripper design and experimental validation workflow [28]-[30].

Based on this background, the present paper develops a complete design-oriented case study using the data and images obtained from the prototype thesis project. The main contributions are: (i) comparison of several ribbed Fin Ray finger geometries; (ii) fabrication of a three finger TPU/PLA prototype using FDM; (iii) integration of an Arduino-based stepper motor drive; and (iv) validation on objects with spherical, cylindrical, and fragile surfaces.

Beyond the development of a functional prototype, this study proposes a complete design workflow integrating CAD modelling, finite element analysis, FDM-based fabrication, and experimental validation. It also compares multiple Fin Ray rib configurations and incorporates analytical design equations to support geometry selection and preliminary performance evaluation. The resulting low-cost platform is readily reproducible and provides a practical basis for both soft-robotics research and engineering education.

ISSN: 2594-1925

2. Design Methodology

The Fin Ray finger is composed of two flexible outer beams connected by a set of internal ribs. The outer boundary is tapered toward the fingertip, forming a triangular or wedge like structure. When the object contacts one side of the finger, the internal ribs redistribute deformation and cause the finger body to curve toward the object. This passive geometric adaptation is suitable for grasping objects whose exact profile is not known in advance.

In this work, the finger design target is not maximum load capacity, but stable and gentle grasping. The finger must therefore satisfy three design requirements: high enough compliance to follow the object surface, sufficient stiffness to prevent slip, and sufficient fatigue resistance for repeated opening and closing cycles. The selected gripper architecture uses three identical fingers equally distributed around the central body to improve centering and increase the total contact area.

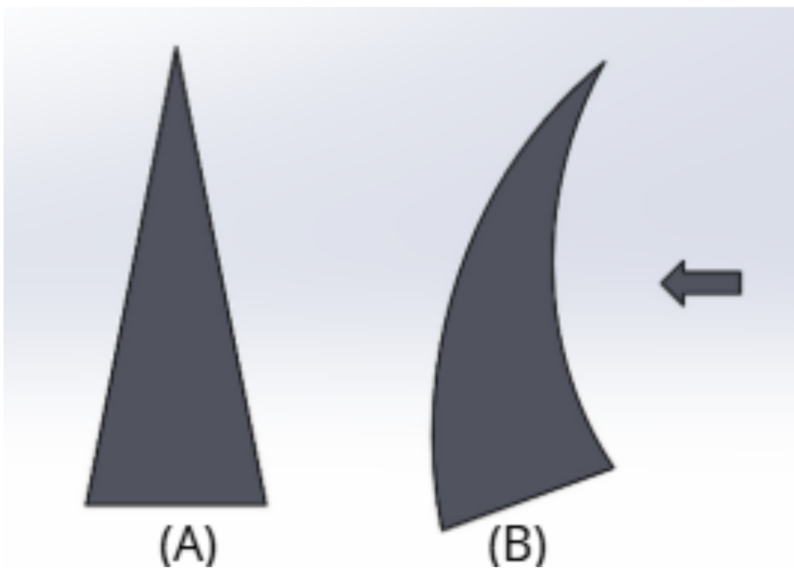

Figure 1. Fin Ray deformation principle used as the basis for the soft finger design.

Table 1. Main materials and functional components of the prototype.

Component	Material	Main role	Key properties used in design
Soft fingers	TPU 95A	Compliant deformation and contact with object	Shore hardness 60-95A; density about 1230 kg/m3; tensile strength 22-55 MPa; elongation at break about 450%
Main body and links	PLA	Structural support and mounting	Density about 1340 kg/m3; tensile strength 50-60 MPa; elastic modulus about 700 MPa; melting point about 220 °C
Actuation unit	Stepper motor + lead-screw/slider linkage	Convert rotation to finger closing motion	Nominal 1.8° step angle; low-cost position control
Control unit	Arduino Uno + A4988 driver	Pulse/direction control of the stepper motor	Simple open loop actuation with adjustable step count

ISSN: 2594-1925

For a journal style design paper, the Fin Ray finger can be idealized as a tapered compliant structure with distributed internal ribs. The local outer width is approximated by a linear taper, while the rib layout controls the equivalent bending stiffness and the direction of passive deformation.

$$w(x) = w_b - \frac{(w_b - w_t)x}{L}; \qquad 0 \le x \le L \quad (1)$$

where w(x) is the local finger width at distance x from the fixed base, w_b and w_t are the finger widths at the base and at the tip, respectively, and L is the effective finger length. The contact location is then expressed in dimensionless form as

$$\lambda = \frac{x_c}{L}; \qquad \lambda \epsilon \left\{\frac{1}{3}, \frac{1}{2} - \frac{2}{3}, \frac{2}{3} - 1\right\} \quad (2)$$

where x_c is the contact position measured from the fixed base and λ is the corresponding dimensionless contact position. The simulation results in the original thesis show that the middle contact region, λ approximately 0.50-0.67, gives the most effective deformation mode because it provides a large contact area without excessive local distortion.

$$k_{eff} = \frac{F_n}{\delta_{tip}}; \quad C_{eff} = \frac{\delta_{tip}}{F_n} = \frac{1}{k_{eff}} \quad (3)$$

where k_{eff} is the effective stiffness of one finger, C_{eff} is the corresponding compliance, F_n is the normal force acting on one finger, and δ_{tip} is the tip displacement. These indicators are useful for comparing different rib geometries under the same nominal normal force.

$$F_n = \frac{F_c}{3} \qquad (4)$$

where F_c is the total commanded or equivalent clamping force of the gripper and F_n is the normal force carried by one finger. Equation (4) assumes that the three identical fingers share the clamping force uniformly, which is appropriate for preliminary sizing and for symmetric objects placed near the centre of the gripper.

The baseline finger has a tapered external profile and internal ribs. The initial geometry was created in SolidWorks and then modified to evaluate the effect of rib orientation and rib distribution. The numerical comparison used a 5 N lateral load applied at several positions along the finger surface. The finger base was fully fixed to reproduce the actual mounting condition in the gripper body.

Three main contact locations were considered: near one-third of the finger length from the base, between one-half and two-thirds of the finger length, and near the fingertip. The simulation results show that the middle contact region provides the best compromise between bending deformation and mechanical stability. This region also corresponds to the expected contact zone when the gripper surrounds objects such as fruit, bottles, or eggs.

To ensure a consistent comparison among different Fin Ray finger configurations, a representative 5 N normal load was applied in all finite element simulations. This load corresponds to the typical grasping force required for

ISSN: 2594-1925

lightweight household objects while remaining within the elastic deformation range of the TPU fingers. The three loading positions were selected to represent contact near the finger base, the primary grasping region, and the fingertip, thereby allowing the deformation behavior to be evaluated over the entire effective working length of the finger under practical grasping conditions.

The compliant fingers were fabricated from TPU 95A because of its excellent flexibility, elastic recovery, and fatigue resistance, making it suitable for repeated bending during grasping. In contrast, PLA was selected for the supporting body owing to its higher stiffness, dimensional stability, and ease of fabrication by fused deposition modelling. The rib geometry, including the inclination angle, spacing, thickness, and curvature radius, was determined according to established Fin Ray design principles and refined through iterative CAD modelling and finite element simulations to achieve an appropriate balance between structural stiffness, deformation capability, and manufacturing feasibility.

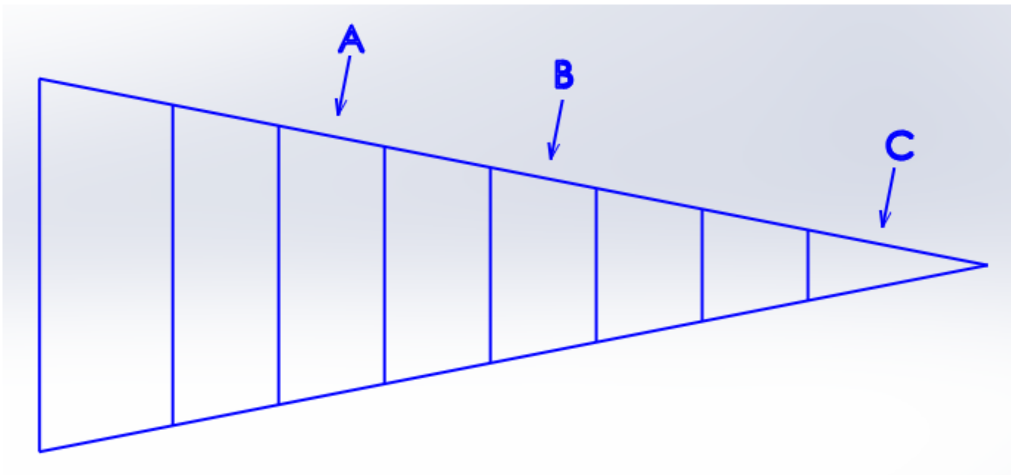

Figure 2. Definition of three representative force application regions along the Fin Ray finger.

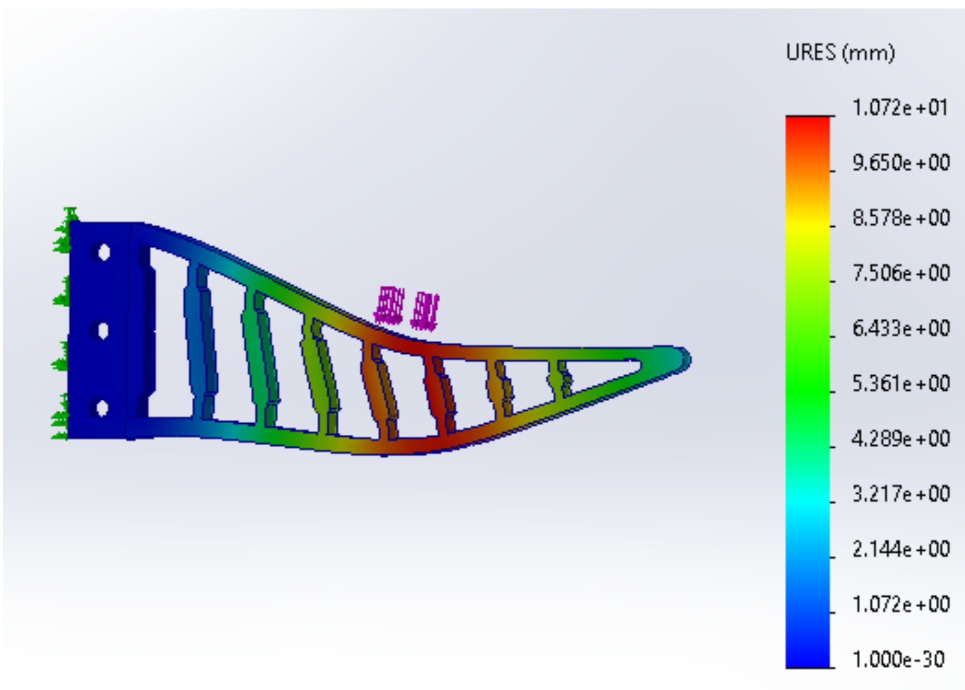

Figure 3. Representative displacement result for the selected middle contact region.

ISSN: 2594-1925

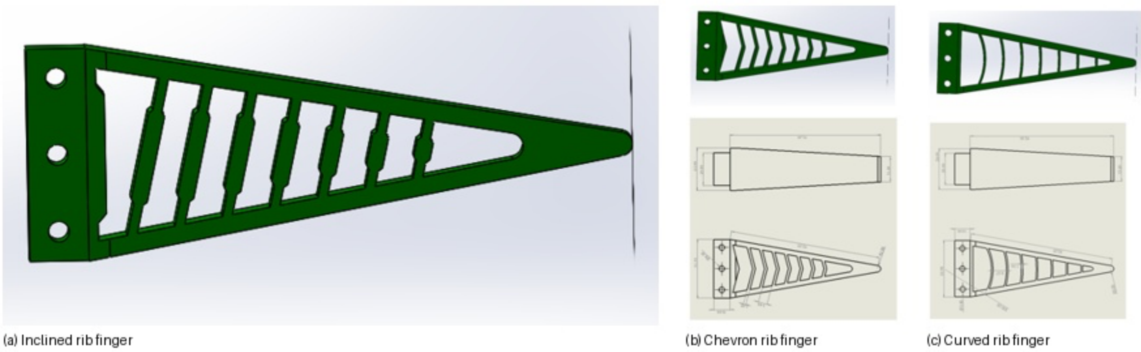

Figure 4. Examples of rib configurations evaluated during the finger design process.

Table 2. Summary of the simulated Fin Ray finger variants.

Finger type	Main rib geometry	Representative design parameters	Main observation
Type 0	Straight ribs approximately parallel to base	Baseline triangular structure	Simple and easy to print; displacement about 10.73 mm in the main middle-contact case
Type 1	Inclined ribs	Rib angle about 12.54°; rib thickness 1.6 mm; spacing about 6 mm	Lower displacement but improved directional deformation; installation orientation becomes important
Type 2	Chevron/folded ribs	Rib angle about 15°; rib thickness 1.6 mm; spacing about 5.44 mm	More uniform force distribution through diagonal ribs and good structural stability
Type 3	Curved ribs	Rib radius about 30 mm; rib thickness about 1.06 mm; spacing about 8.57 mm	Largest displacement in the main case, approximately 14.45 mm, and rapid surface conforming behavior

The SolidWorks simulations were interpreted using the standard finite element equilibrium relation. For each contact case, the base of the finger was fixed and a distributed load was applied on the selected contact region.

$$K(u)u = f; \quad with\ \varepsilon = \frac{1}{2}(\nabla u + \nabla u^T); \quad \sigma = D\varepsilon \qquad (5)$$

where K(u) is the displacement dependent structural stiffness matrix, u is the nodal displacement vector, f is the equivalent nodal force vector, ε is the strain tensor, σ is the stress tensor, and D is the elastic constitutive matrix. The selected design should satisfy both deformation and strength requirements:

$$\delta_{min} \le \delta_{tip} \le \delta_{allow}; \quad and \quad \sigma_{vM} \le \frac{\sigma_y}{SF} \qquad (6)$$

where δ_{min} is the minimum displacement required for surface wrapping, δ_{allow} is the allowable displacement, σ_{vM} is the simulated von Mises stress, σ_y is the material yield or allowable stress, and SF is the design safety factor. The

ISSN: 2594-1925

lower deformation limit ensures sufficient wrapping around the object, while the upper limit and the stress constraint prevent structural failure of the printed TPU finger.

Table 3. Maximum and minimum displacement values extracted from the thesis simulation results.

Case	Type 0 max/min (mm)	Type 1 max/min (mm)	Type 2 max/min (mm)	Type 3 max/min (mm)
TH1	6.263 / 1.253	1.90 / 0.38 to 2.07 / 0.207	2.89 / 0.578	5.1366 / 1.027
TH2	10.73 / 2.145	6.746 / 1.349 to 7.225 / 1.445	8.235 / 1.647	14.45 / 2.891
TH3	11.14 / 2.228	8.303 / 1.661 to 8.755 / 1.751	9.225 / 1.845	14.31 / 2.862

3. Prototype Fabrication and Control System

The final gripper is a three-finger mechanism. The flexible fingers are printed from TPU 95A, while the central body, the finger mounts, and the transmission components are printed from PLA. FDM was selected because it enables rapid iteration of rib geometry and low-cost manufacturing of both rigid and compliant components.

The closing and opening motion is generated by a stepper motor. Motor rotation is transmitted through a central screw/slider mechanism that converts rotation into linear motion. This linear motion moves the linkage system connected to the three fingers, causing the fingers to close for grasping or open for release. The gripper is controlled by an Arduino Uno that sends step and direction signals to an A4988 driver. The driver supplies the stepper motor, while the microcontroller defines the number of pulses and rotation direction.

The required motor torque can be estimated from the axial force demanded by the screw slider mechanism:

$$T_m \geq \frac{F_c p_s}{2\pi \eta_s} \quad (7)$$

where T_m is the required motor torque, F_c is the commanded clamping force, p_s is the screw lead, and η_s is the mechanical efficiency of the screw slider transmission. This equation provides the first order sizing criterion for selecting the stepper motor and checking whether the actuation system can generate the required grasping force.

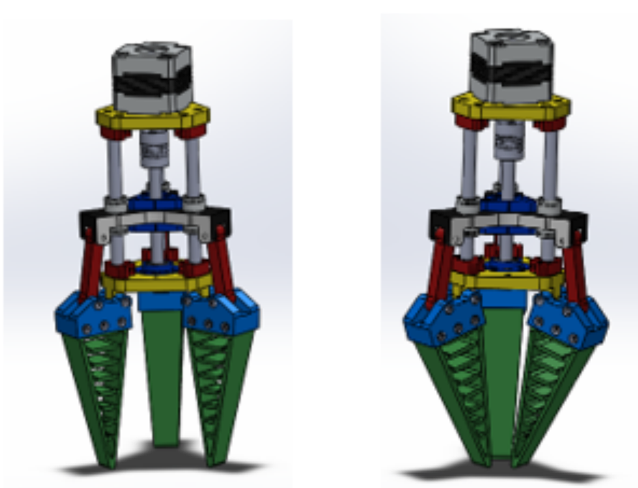

Figure 5. CAD model of the three finger Fin Ray gripper assembly.

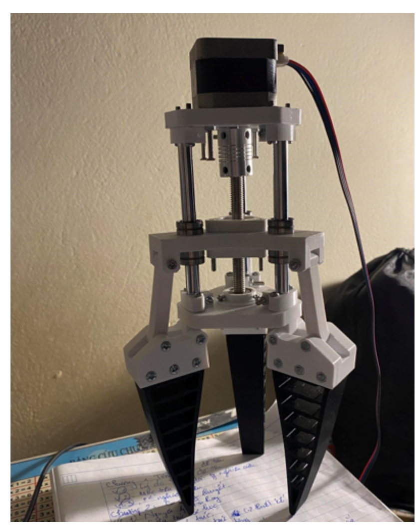

Figure 6. Fabricated prototype of the Fin Ray soft gripper.

ISSN: 2594-1925

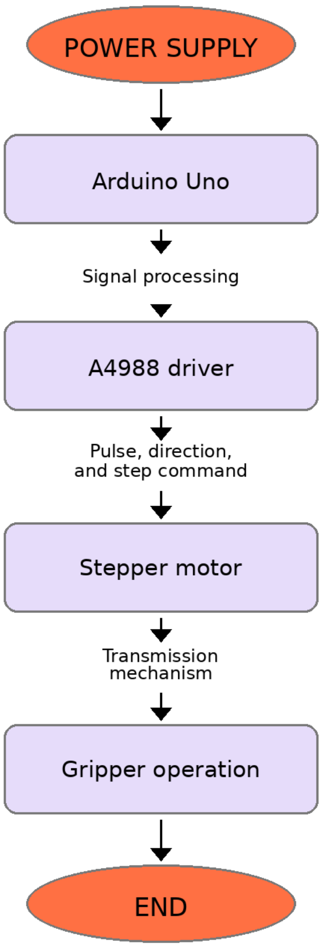

Figure 7. Control flow used for the Arduino based stepper motor actuation.

4. Experimental Evaluation

The prototype was evaluated using three objects selected to represent different grasping conditions. The apple represents a quasi-spherical object with moderate surface stiffness, the plastic bottle represents a cylindrical object, and the egg represents a fragile object requiring low gripping force. For each object, the gripping force was increased gradually, and the grasping condition, curvature radius, and fingertip deflection were recorded. The simulation and experimental curvature results were compared to evaluate the reliability of the design model.

The experimental procedure was conducted by placing the object at the center of the three fingers and increasing the closing command until a stable grasp was achieved. The safe force range was defined as the range in which the object could be held without visible damage or slip.

Each experiment was repeated three times under identical conditions, and the reported values represent the average measurements. Finger deformation was recorded using a fixed-position camera and evaluated through image-based displacement measurements to improve the repeatability of the comparison with the numerical simulations.

ISSN: 2594-1925

Table 4. Experimental objects used to evaluate the gripper.

Object	Geometric representation	Main dimensions	Mass	Purpose of test
Apple	Sphere-like	Diameter 60 mm	240 g	Moderate load spherical grasping
Plastic bottle	Cylinder	Height 200 mm; diameter 60 mm	250 g	Cylindrical grasping with larger height
Egg	Fragile curved body	Diameter about 35 mm	60 g	Low force grasping of damage sensitive object

(a) Apple grasping (b) Bottle grasping (c) Egg grasping

Figure 8. Experimental grasping tests using the fabricated gripper.

The finger curvature radius was treated as the principal validation quantity because it directly reflects the ability of the compliant finger to conform to the object surface. When the deformed finger profile is approximated by a circular arc, the curvature radius can be obtained from the chord length c and sagitta s:

$$R = \frac{c^2+4s^2}{8s} \quad (8)$$

where R is the curvature radius of the deformed finger, c is the chord length of the approximated arc, and s is the sagitta or maximum arc height. The discrepancy between experimental and simulated curvature radius was quantified by the relative error:

$$E_R = \frac{|R_{exp}-R_{sim}|}{R_{sim}} \times 100\% \quad (9)$$

where E_R is the relative curvature radius error, R_{exp} is the experimentally measured curvature radius, and R_{sim} is the simulated curvature radius. The same procedure was applied to the apple, plastic bottle, and egg tests, allowing the model data agreement to be evaluated under different object stiffness and geometry conditions.

For the apple, the gripper was stable over the tested range from 1.5 N to 5.0 N. The measured curvature radius decreased from 213.71 mm at 1.5 N to 54.63 mm at 5.0 N, indicating that a higher clamping force produces stronger wrapping deformation. The simulation experiment error ranged from 1.43% to 9.2%.

For the plastic bottle, the safe gripping range was larger, from 2.0 N to 7.0 N. The curvature radius decreased from 279.40 mm at 2.0 N to 62.65 mm at 7.0 N. The maximum deviation between simulation and experiment was 9.37%, while the minimum error was 0.56%.

ISSN: 2594-1925

For the egg, the allowable force range was limited to 1.0-3.5 N because of the fragile shell. The measured curvature radius decreased from 327.11 mm to 187.61 mm over this range. The maximum error between simulation and experiment was 11.22%, occurring at 2.5 N.

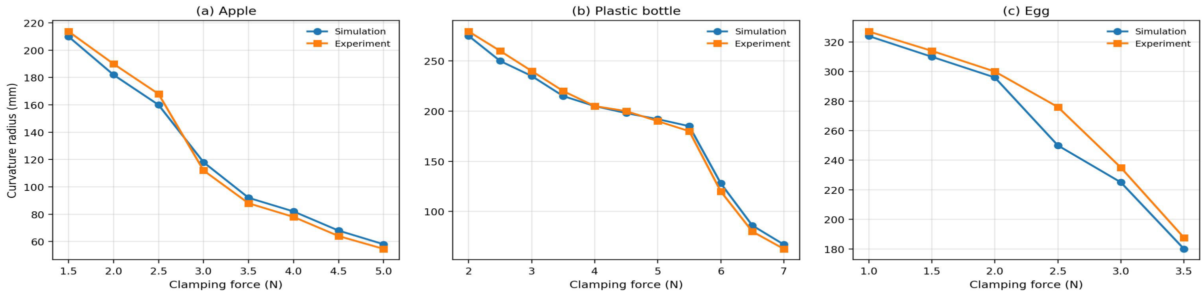

Figure 9. Curvature radius comparison between simulation and experiment for the three test objects.

Table 5. Summary of experimental curvature radius validation.

Object	Safe force range	Curvature radius trend	Simulation experiment error
Apple	1.5-5.0 N	213.71 mm to 54.63 mm	1.43%-9.2%
Plastic bottle	2.0-7.0 N	279.40 mm to 62.65 mm	0.56%-9.37%
Egg	1.0-3.5 N	327.11 mm to 187.61 mm	0.54%-11.22%

For a quasi-static grasp, the minimum condition for holding an object of mass m can be approximated by balancing the available frictional force and the object weight:

$$\mu \sum F_{n,i} \geq mg; \quad i = 1, 2, 3 \qquad (10)$$

where μ is the friction coefficient at the finger object interface, $F_{n,i}$ is the normal force generated by the i th finger, m is the object mass, and g is gravitational acceleration. The safe operating force interval for each object is then defined by

$$\Delta F_{safe} = F_{max} - F_{min} \quad (11)$$

where ΔF_{safe} is the safe operating force interval, F_{min} is the minimum force that prevents slip, and F_{max} is the maximum force before excessive deformation, instability, or possible object damage. A larger ΔF_{safe} indicates a wider operating margin for practical grasping.

The test results confirm the intended behavior of the Fin Ray structure. Increasing the clamping force reduces the curvature radius and increases fingertip deflection, which means that the finger conforms more strongly to the object surface. However, excessive force is undesirable for fragile objects. Therefore, the recommended operating force must be selected according to object stiffness and allowable contact pressure.

The bottle permits the highest tested clamping force because its surface is less fragile and its cylindrical geometry requires stronger lateral retention. The egg requires the lowest force range. The apple represents an intermediate

ISSN: 2594-1925

condition. These results demonstrate that the same three finger architecture can be applied to objects of different geometries if the actuation command is adjusted appropriately.

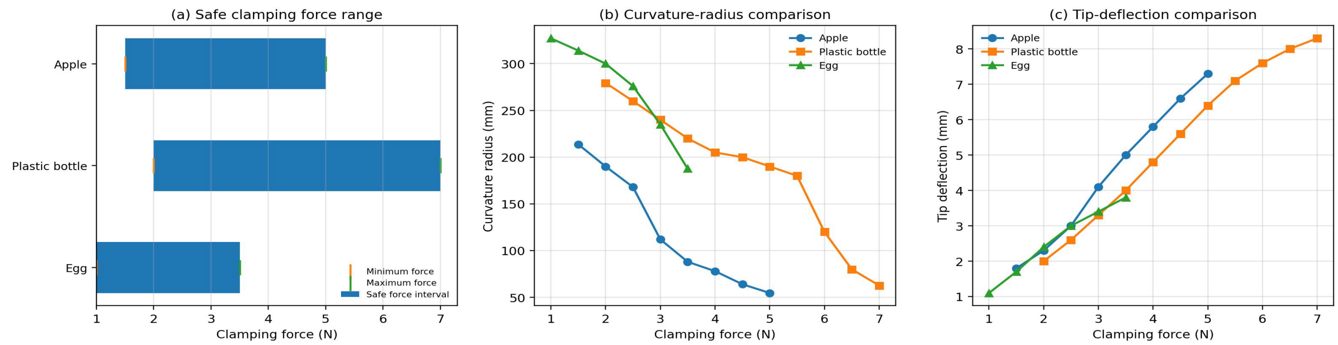

Figure 10. Summary of safe force range, curvature radius, and tip deflection for the three objects.

5. Discussion

The force curvature trend can be represented locally by a linear sensitivity coefficient:

$$S_R = -\frac{\Delta R}{\Delta F_c} \qquad (12)$$

where S_R is the local force curvature sensitivity and $\Delta R/\Delta F_c$ is the change in curvature radius per unit change in clamping force. A larger S_R indicates that the finger curvature changes rapidly with force, which is useful for conformal grasping but may reduce controllability near fragile objects. This explains why the egg required a narrower safe force range than the apple or plastic bottle.

The main design advantage of the proposed gripper is its passive compliance. The mechanical compliance of the ribbed TPU fingers reduces the need for high precision control, because the finger geometry itself contributes to shape adaptation. This characteristic is consistent with the general role of soft robotic grippers in unstructured environments.

The simulation results indicate that rib geometry strongly affects the relationship between displacement and structural stiffness. A highly compliant design provides better surface conformation but may reduce holding force and durability. Conversely, a stiffer rib layout can generate larger grasping force but may reduce the ability to wrap around fragile objects. Therefore, the finger should be selected based on task requirements rather than by maximizing only one metric.

The numerical model adopted several simplifying assumptions to provide an efficient design-oriented evaluation. The printed TPU was modelled as a linear elastic material, while its actual response is inherently hyperelastic under large deformation. In addition, the simulation did not explicitly account for the anisotropic mechanical behaviour introduced by the FDM printing process, variations in friction at the finger-object interface, or nonlinear contact effects during grasping. Furthermore, the prototype employed open-loop stepper-motor actuation without force feedback, limiting the direct validation of contact forces. Although these simplifications may contribute to the discrepancies between simulation and experiment, the overall agreement demonstrates that the proposed model is sufficiently accurate for preliminary design and comparative evaluation. Future work will incorporate hyperelastic constitutive models, anisotropic material properties, nonlinear contact analysis, and closed-loop force sensing to further improve predictive accuracy.

ISSN: 2594-1925

The experimental errors between simulation and measurement are acceptable for a low-cost prototype, but several factors can explain the remaining difference: simplified material properties in SolidWorks, anisotropy caused by FDM printing, friction variation at the object finger interface, manual measurement error of curvature radius, and open loop stepper motor actuation. Future work should include hyperelastic material characterization of printed TPU, repeatability testing over many cycles, closed loop force or tactile feedback, and optimization of rib geometry using a multi objective framework.

6. Conclusion

A three finger Fin Ray soft gripper was designed, fabricated, and experimentally evaluated. The soft fingers were printed from TPU 95A and mounted on a PLA body actuated by a stepper motor. SolidWorks simulations showed that the most effective contact region is located between one half and two thirds of the finger length from the base. Among the tested rib configurations, the curved rib finger provided the largest displacement in the main contact case, reaching approximately 14.45 mm.

The fabricated prototype successfully grasped an apple, a plastic bottle, and an egg. Stable grasping was achieved within force ranges of 1.5-5.0 N, 2.0-7.0 N, and 1.0-3.5 N, respectively. The curvature radius validation showed reasonable agreement between simulation and experiment, with maximum reported error of 11.22%.

In addition to validating the proposed prototype, this work establishes a reproducible CAD–FEA–fabrication–experiment framework for Fin Ray gripper development. The comparison of different rib configurations, together with the proposed analytical design equations and experimental validation, provides practical guidelines for future soft-gripper design while offering an accessible low-cost platform for research and laboratory teaching.

The results demonstrate the feasibility of a low-cost Fin Ray gripper for adaptive handling of objects with different shapes and fragility levels.

7. Authorship acknowledgments

Hoang Bui Huy: Conceptualization; Methodology; Investigation; Resources ; Data Analysis; Validation; Writing – Review and Editing.

References

[1] D. Rus and M. T. Tolley, “Design, fabrication and control of soft robots,” Nature, vol. 521, no. 7553, pp. 467-475, May 2015, doi: 10.1038/nature14543.

[2] S. Kim, C. Laschi, and B. Trimmer, “Soft robotics: A bioinspired evolution in robotics,” Trends Biotechnol., vol. 31, no. 5, pp. 287-294, May 2013, doi: 10.1016/j.tibtech.2013.03.002.

[3] C. Laschi, B. Mazzolai, and M. Cianchetti, “Soft robotics: Technologies and systems pushing the boundaries of robot abilities,” Sci. Robot., vol. 1, no. 1, Art. no. eaah3690, Dec. 2016, doi: 10.1126/scirobotics.aah3690.

[4] C. Majidi, “Soft-matter engineering for soft robotics,” Adv. Mater. Technol., vol. 4, no. 2, Art. no. 1800477, Feb. 2019, doi: 10.1002/admt.201800477.

[5] J. Shintake, V. Cacucciolo, D. Floreano, and H. Shea, “Soft robotic grippers,” Adv. Mater., vol. 30, no. 29, Art. no. 1707035, Jul. 2018, doi: 10.1002/adma.201707035.

[6] W. Crooks, S. Rozen-Levy, B. Trimmer, C. Rogers, and W. Messner, “Fin Ray Effect inspired soft robotic gripper: From the RoboSoft Grand Challenge toward optimization,” Front. Robot. AI, vol. 3, Art. no. 70, Nov. 2016, doi: 10.3389/frobt.2016.00070.

[7] Y. Yang, K. Jin, H. Zhu, G. Song, H. Lu, and L. Kang, “A 3D-printed Fin Ray Effect inspired soft robotic gripper with force feedback,” Micromachines, vol. 12, no. 10, Art. no. 1141, Sep. 2021, doi: 10.3390/mi12101141.

ISSN: 2594-1925

[8] G. L. Srinivas, A. Javed, and L. M. Faller, "Versatile 3D-printed fin-ray effect soft robotic fingers: Lightweight optimization and performance analysis," J. Braz. Soc. Mech. Sci. Eng., vol. 46, Art. no. 382, May 2024, doi: 10.1007/s40430-024-04957-0.
[9] F. Varghese, F. Auat-Cheein, and M. Koskinopoulou, "Finite element optimization of a flexible fin-ray-based soft robotic gripper for scalable fruit harvesting and manipulation," Smart Agric. Technol., vol. 11, Art. no. 100899, Aug. 2025, doi: 10.1016/j.atech.2025.100899.
[10] X. Shan and L. Birglen, "Modeling and analysis of soft robotic fingers using the Fin Ray effect," Int. J. Robot. Res., vol. 39, no. 14, pp. 1686-1705, Dec. 2020, doi: 10.1177/0278364920913926.
[11] X. Wang, J. J. Dabrowski, J. Pinskier, L. Liow, V. Viswanathan, R. Scalzo, and D. Howard, "PINN-Ray: A physics-informed neural network to model soft robotic Fin Ray fingers," in Proc. IEEE/RSJ Int. Conf. Intell. Robots Syst. (IROS), 2024, pp. 247-254, doi: 10.1109/IROS58592.2024.10802217.
[12] Q. Cong, W. Fan, and D. Zhang, "TacFR-Gripper: A reconfigurable Fin-Ray-based gripper with tactile skin for in-hand manipulation," Actuators, vol. 13, no. 12, Art. no. 521, Dec. 2024, doi: 10.3390/act13120521.
[13] Z. Deng and M. Li, "Learning optimal Fin-Ray finger design for soft grasping," Front. Robot. AI, vol. 7, Art. no. 590076, Feb. 2021, doi: 10.3389/frobt.2020.590076.
[14] K. Elgeneidy, P. Lightbody, S. Pearson, and G. Neumann, "Characterising 3D-printed soft Fin Ray robotic fingers with layer jamming capability for delicate grasping," in Proc. 2nd IEEE Int. Conf. Soft Robot. (RoboSoft), Seoul, Republic of Korea, 2019, pp. 143-148, doi: 10.1109/ROBOSOFT.2019.8722715.
[15] R. L. Truby and J. A. Lewis, "Printing soft matter in three dimensions," Nature, vol. 540, no. 7633, pp. 371-378, Dec. 2016, doi: 10.1038/nature21003.
[16] T. J. Wallin, J. Pikul, and R. F. Shepherd, "3D printing of soft robotic systems," Nat. Rev. Mater., vol. 3, pp. 84-100, Feb. 2018, doi: 10.1038/s41578-018-0002-2.
[17] F. Schmitt, O. Piccin, L. Barbe, and B. Bayle, "Soft robots manufacturing: A review," Front. Robot. AI, vol. 5, Art. no. 84, Jul. 2018, doi: 10.3389/frobt.2018.00084.
[18] G. M. Whitesides, "Soft robotics," Angew. Chem. Int. Ed., vol. 57, no. 16, pp. 4258-4273, Apr. 2018, doi: 10.1002/anie.201800907.
[19] F. Ilievski, A. D. Mazzeo, R. F. Shepherd, X. Chen, and G. M. Whitesides, "Soft robotics for chemists," Angew. Chem. Int. Ed., vol. 50, no. 8, pp. 1890-1895, Feb. 2011, doi: 10.1002/anie.201006464.
[20] P. Polygerinos et al., "Modeling of soft fiber-reinforced bending actuators," IEEE Trans. Robot., vol. 31, no. 3, pp. 778-789, Jun. 2015, doi: 10.1109/TRO.2015.2428504.
[21] A. D. Marchese, R. K. Katzschmann, and D. Rus, "A recipe for soft fluidic elastomer robots," Soft Robot., vol. 2, no. 1, pp. 7-25, Mar. 2015, doi: 10.1089/soro.2014.0022.
[22] R. Deimel and O. Brock, "A novel type of compliant and underactuated robotic hand for dexterous grasping," Int. J. Robot. Res., vol. 35, no. 1-3, pp. 161-185, Jan. 2016, doi: 10.1177/0278364915592961.
[23] E. Brown et al., "Universal robotic gripper based on the jamming of granular material," Proc. Natl. Acad. Sci. U.S.A., vol. 107, no. 44, pp. 18809-18814, Nov. 2010, doi: 10.1073/pnas.1003250107.
[24] M. Cianchetti, C. Laschi, A. Menciassi, and P. Dario, "Biomedical applications of soft robotics," Nat. Rev. Mater., vol. 3, pp. 143-153, Jun. 2018, doi: 10.1038/s41578-018-0022-y.
[25] M. Manti, V. Cacucciolo, and M. Cianchetti, "Stiffening in soft robotics: A review of the state of the art," IEEE Robot. Autom. Mag., vol. 23, no. 3, pp. 93-106, Sep. 2016, doi: 10.1109/MRA.2016.2582718.
[26] J. Hughes, U. Culha, F. Giardina, F. Guenther, A. Rosendo, and F. Iida, "Soft manipulators and grippers: A review," Front. Robot. AI, vol. 3, Art. no. 69, Nov. 2016, doi: 10.3389/frobt.2016.00069.
[27] L. Hines, K. Petersen, G. Z. Lum, and M. Sitti, "Soft actuators for small-scale robotics," Adv. Mater., vol. 29, no. 13, Art. no. 1603483, Apr. 2017, doi: 10.1002/adma.201603483.
[28] S. Terryn, J. Brancart, D. Lefeber, G. Van Assche, and B. Vanderborght, "Self-healing soft pneumatic robots," Sci. Robot., vol. 2, no. 9, Art. no. eaan4268, Aug. 2017, doi: 10.1126/scirobotics.aan4268.
[29] R. Chen et al., "Bio-inspired shape-adaptive soft robotic grippers augmented with electroadhesion functionality," Soft Robot., vol. 6, no. 6, pp. 701-712, Dec. 2019, doi: 10.1089/soro.2018.0120.
[30] S. Terrile, M. Arguelles, and A. Barrientos, "Comparison of different technologies for soft robotics grippers," Sensors, vol. 21, no. 9, Art. no. 3253, May 2021, doi: 10.3390/s21093253.

ISSN: 2594-1925

Copyright (c) 2026 Hoang Bui Huy

This text is protected by a Creative Commons 4.0. license.

You are free to share—copy and redistribute the material in any medium or format—and adapt the document—remix, transform, and build upon the material—for any purpose, even commercially, provided you comply with the following condition:

Attribution: You must give appropriate credit to the original work, provide a link to the license, and indicate if changes were made. You may do so in any reasonable manner, but not in any way that suggests the licensor endorses you or your use of the work.

License summary - Full license text

ISSN: 2594-1925